Inconsistency of threat level in soft armour standards, correlation of experimental tests to bullet X-ray 3D images.

John Thornby [1], Dirk Landheer [2], Tim Williams [2], Jane Barnes-Warden [3], Paul Fenne [3], Alex Attridge [1], Mark A. Williams [1]

[1] *WMG, University of Warwick, CV4 7AL, United Kingdom*
john.thornby@warwick.ac.uk
[2] *Simpact Engineering Ltd, 22 New Street, Leamington Spa, Warwickshire, CV31 1HP, United Kingdom*
[3] *Metropolitan Police Service, Operational Technology, 8-20 Loman Street, SE1 0EH, United Kingdom*

Abstract. Fundamental to any ballistic armour standard is the reference projectile that is to be defeated. Typically, for certification, consistency of bullet geometry is assumed. Therefore, practical variations in bullet jacket dimensions can have far reaching consequences. Traditionally, internal dimensions have been analysed by physically sectioning bullets – an approach which rules out any subsequent ballistic assessment. The use of a non-destructive X-ray Computed Tomography (CT) method was demonstrated in [1]. Now, the authors apply this technique to correlate bullet impact response to jacket thickness variations. A set of 20 bullets (9 mm DM 11) was selected to analyse both intra and inter bullet variations using an image based analysis method to map the jacket thickness and measure the centre of gravity. Thickness variations of the order of 200μm were found commonly across all the bullets along the length and an angular variation of up to 50μm was found in a few bullets. The bullets were subsequently impacted against a rigid flat plate and re-scanned. The results of the experiments are shown and compared to the un-deformed bullet jacket thickness variations. The conclusions are relevant for future soft armour standards and provide important data for numerical model correlation and development.

1. INTRODUCTION

Jacketed bullets typically contain a certain mass of heavy metal, such as lead, encased within a metal sleeve – the jacket. The jacket helps to reduce the friction of the rifle/gun barrel and to carry the lead core intact to the target, while the mass of the lead helps to deliver maximum kinetic energy for a given firing velocity. A bullet's jacket might deform or rupture depending on the velocity of impact and nature of the target. Its thickness also plays a definite role in the manner in which it deforms when impacting a target.

Measurement of jacket thickness variation is useful in the development of accurate ballistic performance simulations using numerical analysis methods, which currently use only the gross geometry of bullets. It has long been asserted that jacket thickness is a major contributor to bullet fragmentation and penetration power [2]; however no major modelling work to date has attempted to account for its impact on ballistic performance as such models would be difficult to validate in the absence of a reliable method to measure jacket thickness variations non-destructively both pre- and post-impact. In addition, measurement of jacket thickness helps quality tests and forensic investigations required for qualifying and identifying bullets from different manufacturers.

Many methods of measuring the physical parameters of bullets have been documented. Destructive testing reveals detailed information regarding jacket thickness [3], however such methods are restrictive, may introduce inaccuracies due to deformation and preclude studying geometric features of a bullet both pre- and post-impact. Although non-destructive radiographic techniques have been employed [4-7], they have not been exploited to their fullest potential. X-ray radiography lends itself to estimation of jacket thickness in a 2D plane; however, it cannot capture 3D geometry. X-ray Computed Tomography (CT) is a natural extension of X-ray radiography and possesses the capability to analyse geometry in detail through the reconstruction of a three-dimensional volume.

This paper presents the application of X-ray CT [8] for the extraction of the bullet geometry both before and after impact. Following the method prescribed in [1] (summarised in Section 2.), a set of 20, nominally identical, bullets were CT scanned prior to being subjected to ballistic performance tests under controlled conditions. The deformed projectiles were then re-scanned in order to observe and quantify the

degree of deformation resulting from the impacts, with a view to correlating these ballistic performance indicators with geometric features of the un-deformed bullets prior to impact. This data will be used going forward to assist in the creation and validation of finite element models to more accurately describe ballistic impacts and help quantify the variability of threat level of ammunition of this kind.

2. CT SCANNING AND IMAGE ANALYSIS

Computed Tomography is a method of three-dimensional image reconstruction of an object from a number of 2D X-ray images (radiographs), taken at different angles. X-ray attenuation is dependent on the density and thickness of the object through which the beam has passed, so each projection image encodes information about the nature of the material in the volume. With sufficiently many projections, one may use numerical reconstruction algorithms to disentangle this volume information and create a digital 3D representation of the volume. With appropriate X-ray conditions and post-processing methods, a volume element (voxel) resolution of below 10 microns is tenable.

2.1 CT scanning

A Nikon Metrology XTH 320 LC system was used for this study. This is an industrial micro-focus CT scanner with a 320 kV X-ray tube and a 2000 × 2000 pixel detector panel. Bullets were scanned using an appropriate electron acceleration voltage and a copper filter to exclude low energy X-rays, which prevents detector saturation and helps mitigate beam hardening effects which can cause artefacts in the reconstructed volume. A full discussion of this procedure and subsequent analysis is provided in [1, 9]. All bullets were scanned prior to ballistic testing (Section 3) and then re-analysed using an identical method.

2.2 Bullet volume reconstruction and jacket segmentation

Three-dimensional volume data is reconstructed from radiograph images (Figure 1a) using Nikon Metrology's proprietary software, *CT Pro*. Severe X-ray attenuation due to the density of material in the lead core of the bullets results in beam hardening, which is partially corrected for by a built-in algorithm in *CT Pro*. A noise filtering algorithm is also available to extract volume elements from background.

The reconstructed volume is visualised in Volume Graphics' *VG Studio Max*. Volume data is first passed through a median filter which smoothes the images, facilitating the use of built-in algorithms to select regions of interest (ROIs). ROIs are established for the "jacket" and the "core" of the bullet using a region growing tool which selects voxels with similar grey values that lie within a certain radius of a given seed point (Figure 1b). The bright halo (caused by beam hardening within the lead core) provides a natural demarcation of the jacket and core. A 3D morphological closing operation is then performed on the ROI which fills in holes and discontinuities and also removes any sharp corners. Once segmented, the ROIs can be rendered (Figure 1c) and 2D slices extracted in grayscale for further analysis (Figure 1d).

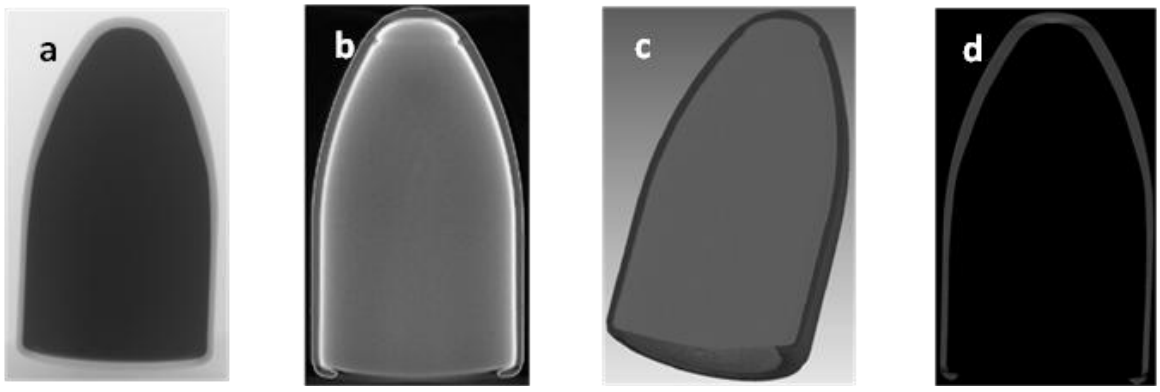

Figure 1. (a) a radiograph image of a bullet; (b) segmentation of a bullet jacket using a region growing algorithm and morphological operations; (c) 3D rendering of a complete bullet; (d) isolated jacket 2D slice.

2.3 Image analysis methodology

2.3.1 Extracting image slices

A cylinder is fitted to points selected randomly from the circumference of the jacket near the base of the bullet. This cylinder is used to verify the CT reconstruction scaling and as a geometrical reference, so that when the volume images are exported they are aligned consistently rather than to some arbitrary global coordinate frame. The cylinder axis therefore defines the orientation of the bullet and also a base plane, which can be taken as a reference for subsequent centre of gravity (COG) calculations. The jacket volume is then divided into slices one voxel thick perpendicular to the reference axis, resulting in a series of 2D greyscale cross-sectional images in which the bullet jacket material is evident as a grey ring against a black background. This image stack is exported for analysis and the procedure is repeated for the whole bullet (containing the lead core as well).

2.3.2 Establishing a physical reference

In this study, only bullet impacts without visible tumbling are considered. In order to compare jacket geometry variations before and after impact, a common coordinate system must be established. Three small notches and a double notch are physically carved on the underside of the bullet jacket at the cardinal points and are visible in the reconstructed CT image slices. Imaginary lines connecting diametrically opposite notches define a reference axis system, and their intersection is taken as the central reference point about which all angular measurements are made (with the double notch taken as 0°). Since the notches are visible in both pre- and post-impact reconstructed images, one can reliably construct the same coordinate system for both cases and hence reproducibly establish the bullet orientation.

2.3.3 Calculation of jacket thickness

An analysis tool has been developed in-house to calculate the jacket thickness. The image slice stack is first loaded into computer memory and a cross sectional profile at 0° is computed from the 3D stack of images. This profile will have jagged edges due to inherent noise variations, so these are smoothed using morphological operations to flatten out small projected points and fill tiny undercuts on the profile image boundary. Binary images are obtained by thresholding and a parametric least squares Bezier curve fitting algorithm is employed to define the internal and external boundaries of the bullet profile image. The distance, normal to the outer boundary, is calculated analytically between these curves at sample points along the length of the bullet and corresponds to the jacket thickness. This procedure is repeated for profiles at other (discrete) angles until the whole surface of the bullet has been analysed. The reader is referred to [1] for a thorough discussion of the accuracy and validity of this method.

To visualise the jacket thickness, a 2D Cartesian colour map representation is adopted. Position coordinates on the map are the external length of the bullet jacket profile (from the tip) and the radial angle of that profile (relative to the bullet coordinate system); i.e. a pixel (x,y) on the map is a distance x from the tip of the bullet along the edge, at a radial angle y and is coloured according to the jacket thickness.

2.3.4 *Calculation of centre of gravity*

The COG is calculated using the relative weights of each voxel within the reconstructed volume, assuming densities of 11340 kg/m^3 for lead and 7870 kg/m^3 for the steel jacket. A second set of image slices are read into computer memory, containing both the jacket and the lead core. Logical image operations are carried out to identify the pixels corresponding to jacket material and lead, which are then weighted accordingly to numerically ascertain the position of the COG, C_x, C_y and C_z, relative to the reference plane defined previously. It is then a trivial calculation to derive the position of the COG relative to the tip of the bullet.

3. BALLISTIC TESTING

20 DM11 bullet heads from two different manufacturers (15 RWS and 5 GM) were tested at Hallrite Precision Engineering ballistic range in Chesterfield, Derbyshire (UK). The objective of the tests was to

generate pairs of bullets, deformed by ballistic collision under identical conditions, to be compared in detail with the Micro CT scanner at WMG for subsequent use in ballistic impact modelling at Simpact.

A flat, hardened steel plate target was chosen in order to eliminate variation in target performance and produce bullet deformations that were characteristic of (or as close to as possible) the typical mushroom type deformation seen within soft armour. A standard configuration was used to fire the bullets via a remotely operated breach. Figure 2 (left) shows the experimental setup including the painted steel plate; a High Speed Video (HSV) camera and 3 lighting units. The HSV had a close to square-on view of the target, facilitating imaging the bullets perpendicular to their direction of motion, shown in Figure 2 (right). The level of light generated allowed for a good depth of field and an appropriate frame rate of 28000fps. A small magnetic rule was attached to the strike face adjacent to the impact zone for reference.

Figure 2. Experimental setup (left): The ballistic target is a flat, hardened steel plate. Three lighting units provide necessary illumination for a High Speed Video (HSV) camera which captures the impact (right).

Bullet velocity measurement was provided by the range chronograph and verified with the High Speed Video. Previous experience with this setup suggested that a relatively low impact velocity of around 100m/s was required to give representative bullet deformations. In order to attain these velocities, a relatively small amount of propellant charge (~2.5 grains) was required. In this regime, however, low pressures within the bullet casing and friction effects in the breach become predominant, resulting in a challenge to produce consistent impact velocities. To mitigate the problem, a foam 'filler' material was placed above the powder in each shot to give a consistent powder distribution and encourage even combustion. Nevertheless, a significant spread of bullet velocities was observed and on one occasion a misfire occurred. Bullet impact velocities are tabulated in Table 1 and Figure 3 illustrates the bullet heads. Bullets 11-15 (red box) are the GM specification and the rest are RWS. It can be seen that the GM spec provided more consistent bullet velocities and deformation.

Bullet #	Manufacturer	Velocity (m/s)	Bullet #	Manufacturer	Velocity (m/s)
11	GM	116.8	21	RWS	Misfire
12	GM	112.0	22	RWS	147.9
13	GM	114.0	23	RWS	153.8
14	GM	116.3	24	RWS	127.0
15	GM	120.8	25	RWS	139.9
16	RWS	134.8	26	RWS	153.8
17	RWS	123.2	27	RWS	145.3
18	RWS	146.1	28	RWS	143.4
19	RWS	130.2	29	RWS	156.4
20	RWS	150.8	30	RWS	102.8

Table 1. Manufacturer and velocity information for each bullet in the study (bullets 1-10 were test shots). Shaded cells represent groups of bullets selected for comparison.

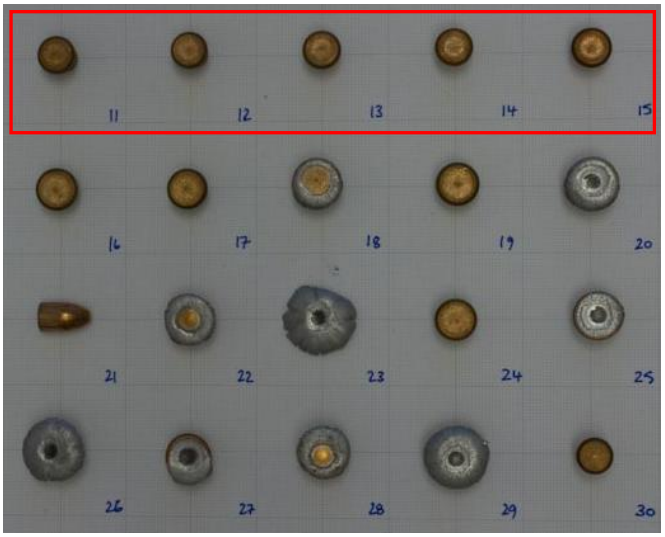

Figure 3. Bullets 11-30 (post-impact), demonstrating the degree of variation in deformation. The top row (red box) are GM specification and the rest are RWS.

4. OBSERVATIONS & ANALYSIS

The bullets were retrieved and identified for close inspection and CT scanning at WMG. For comparative assessment, bullets 11, 14 and 15 were chosen from the GM specification because they had very similar impact velocities. Their consistent ballistic performance may be ascribed to their physical dimensions, which seem to be more compatible with the shell casings used in the ballistic test series. All five GM bullets had a measured diameter of 9.00 mm, implying a tighter fit within the case than the RWS bullets, which measured 8.98 mm. It is speculated that this goodness of fit leads to more consistent pressure within the casing. Furthermore, a black powder residue was found on some of the RWS casings.

Figure 4 shows the three deformed GM bullet heads side by side. It can be seen that they exhibit very similar overall deformation. The flat face of each impacted bullet head shows a concentric ring of lighter colour. This is believed to be the thicker ring of jacket material described in Section 4.1. Bullets 16 and 17 were also chosen from the RWS bullet samples, due to the similarity of their deformation.

Figure 4. Post-impact bullet heads 11 (116.8 m/s), 14 (116.3 m/s) and 15 (120.8 m/s), GM specification.

4.1 Pre-impact comparison

Figure 5 shows the jacket thickness colour plot for bullet 11, prior to ballistic impact. For clarity, the Cartesian plot (described in Section 2.3.3) is shown alongside a polar representation. This data is representative of the other bullets in the sample and overall jacket thickness variations have a similar distribution to those reported by Kumar et al [1] – although with a greater variation towards the tip of the bullet. The same interesting 'ring' feature near the tip is present in all of the GM bullets, visualised as a red

band in the thickness plot. The red equates to 525µm jacket thickness locally, compared to approximately 400 µm at the tip and shoulder.

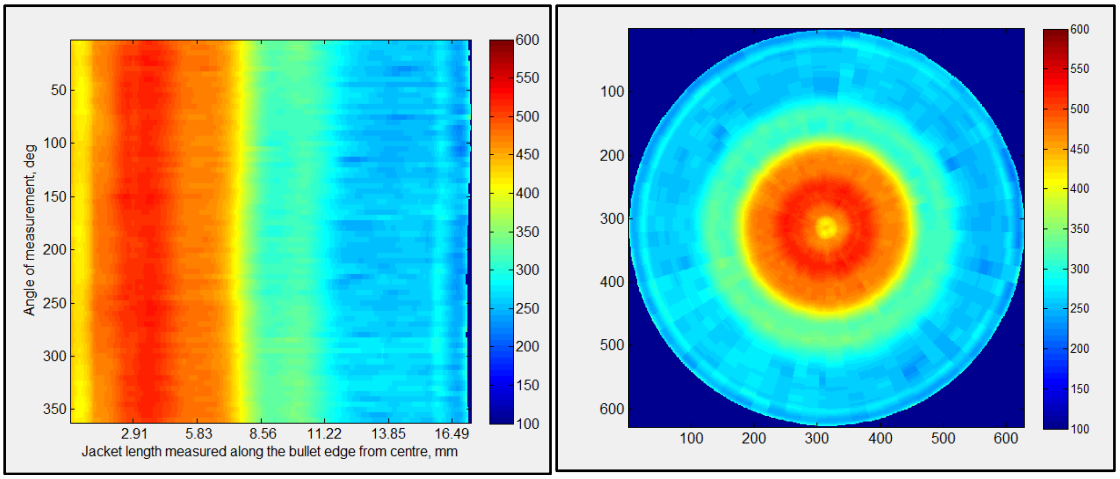

Figure 5. Pre-impact jacket thickness colour plots for bullet 11: Cartesian representation (left) and polar representation (right). All jacket thicknesses are measured in µm.

In bullets 14 and 15, the ring pattern is noticeably thicker by around 100µm; the tip of bullet 11 is thinner by around 100µm and the rear section of bullet 11 is thinner by around 70µm, shown in Figure 6 (Cartesian plots for bullets 14 and 15 can be found in Figure 11 & Figure 12). A comparison of intra-bullet jacket thickness for bullets 11, 14 and 15 is shown in Table 2. It can be seen that there is an angular variation in jacket thickness of order 50µm at equivalent positions along a bullet's length.

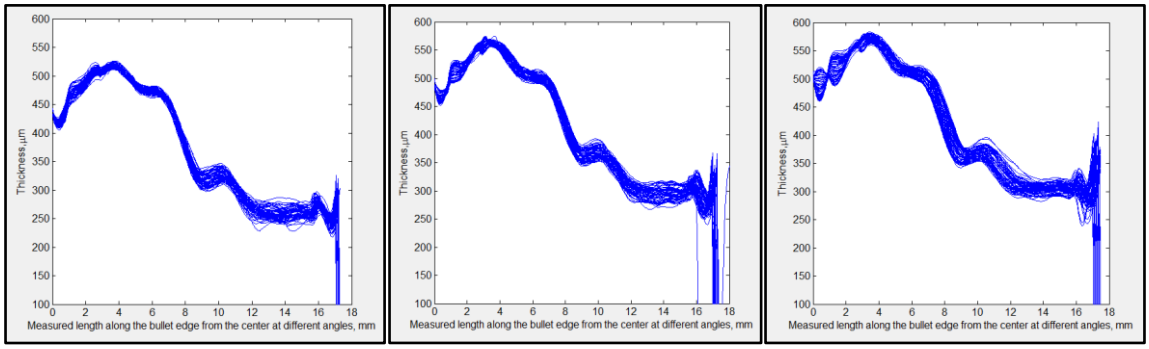

Figure 6. Jacket thickness variation (µm) for bullets 11 (left), 14 (centre) and 15 (right), pre-impact. Lines represent the thickness profiles at different radial angles around the bullet. A spread of as much as 50 µm is observed at equivalent positions along the bullets' length.

Length Position	0mm	2mm	4mm	6mm	8mm	10mm	12mm	14mm
Mean jacket thickness angular variation (µm)	16.7	43.1	32.0	36.1	51.4	44.4	52.8	54.2

Table 2. Mean intra-bullet jacket thickness angular variation (µm), pre-impact.

4.2 Post-impact comparison

The following sequence of events has been identified in the deformation of the bullet:

1. The bullet tip contacts the target. The contact generates normal stress, locally thinning the jacket. See schematic representation Figure 7.
2. A combination of radial compressive stress and tangent tensile stress results in flattening of the tip. See schematic representation Figure 7.
3. An internal pressure wave starting at the tip from the relatively soft lead core causes tangent tensile stress in the jacket, stretching the diameter. Where the jacket is in contact with the target, friction counteracts this stretching, see illustration Figure 8. The edge of the contact zone, not the area of largest diameter change, is where ultimately rupture of the jacket will occur if the impact velocity is high enough. This is supported by Figure 3. In case of impact with a soft target such as soft armour, rupture is most likely to occur in the zone that undergoes the largest diameter change.

Figure 7. Stage 1 (left), Stage 2 (right)

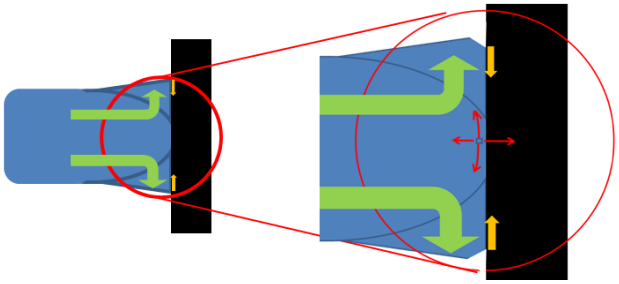

Figure 8. Stage 3

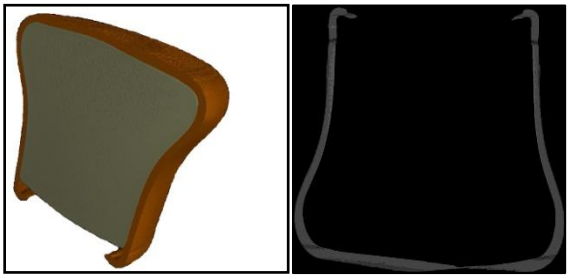

Figure 9. 3D view of a section through the CT data of a deformed bullet and cross section of bullet 14

In the experiments, elongations exceeding 100% were observed. This is only possible as a result of the multi axial stress condition. By nature, the pressure load in a cylinder can cause unstable behaviour dependant on material hardening properties. Any irregularities in wall thickness along the circumference of the jacket can trigger instability, ultimately resulting in rupture. Figure 9 shows an example of a cross section of the CT data for a deformed bullet (left) and a slice of bullet 14 at the point at which the jacket thickness has thinned the most (90º).

The change in distance of the centre of gravity (COG) to the tip of the projectile is a measure of the mechanical compliance. A larger compliance typically relates to a reduction in penetrative power. Table 3 summarises physical properties including COG for the 3 GM and the 2 RWS bullets. For bullet 11 the COG position moves forward by 5.36mm whereas in bullet 14 it moves forward by 5.15mm. This increase of 0.21mm in forward deformation is thought to be due to the lower jacket thickness observed in bullet 11

(given the same mass and impact velocity). For bullet 15, the COG position moved by a further 0.26mm and this considered to be most likely due to the higher impact velocity (+7% kinetic energy).

Bullet	Pre-impact			Post-impact		
	Mass (g)	Length (mm)	COG, C_z (mm)	Mass (g)	Length (mm)	COG, C_z (mm)
11	8.0088	15.80	8.99	8.0083	10.49	3.63
14	8.0251	15.80	9.05	8.0244	10.50	3.90
15	8.0203	15.91	9.13	8.0196	10.19	3.30
16	8.0114	15.84	9.23	8.0105	8.51	
17	7.9992	15.62	8.73	7.9978	9.12	

Table 3. Physical properties of the bullets pre- and post- impact. Length is measured (with a screw gauge micrometer) from the tip of the bullet to the base of the lead core. C_z is the distance of the z-component of the COG from the bullet tip, calculated from the CT scan voxel weightings .

Figure 10, Figure 11 and Figure 12 show the un-deformed and deformed Cartesian plots for the GM bullet heads 11, 14 and 15 respectively. All three of the deformed plots show distinct areas of thinning and it is believed that these areas would be the first areas of rupture if the bullet continued to deform. There is a weak correlation between the area of thinning in the deformed bullets and the pre-impact jacket thickness distribution. In bullet 14 and 15 the 'ring' is disrupted in thickness in this area and this may have led to the pronounced jacket thinning in the deformed bullet.

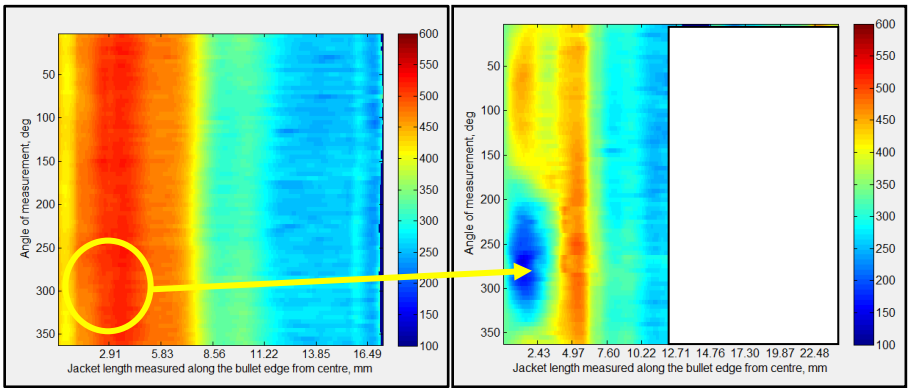

Figure 10. Cartesian thickness plot in μm for Bullet 11, pre-impact (left), post-impact (right)

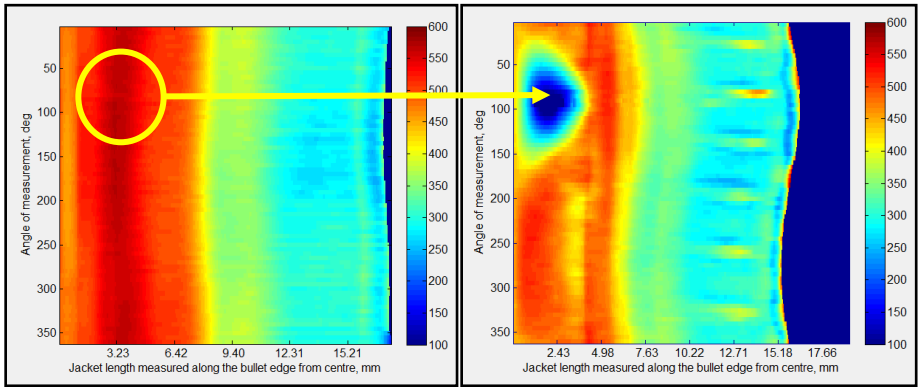

Figure 11. Cartesian thickness plot in μm for Bullet 14, pre-impact (left), post-impact (right)

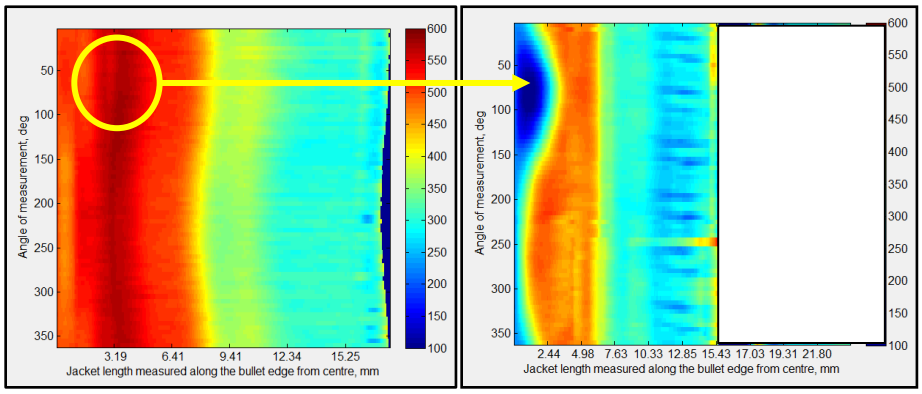

Figure 12. Cartesian thickness plot in μm for Bullet 15, pre-impact (left), post-impact (right)

Figure 13 and Figure 14 show the Cartesian and polar jacket thickness plot for the RWS bullet heads 16 & 17. The white rectangular boxes within the Cartesian plots contain incomplete data and are therefore disregarded.

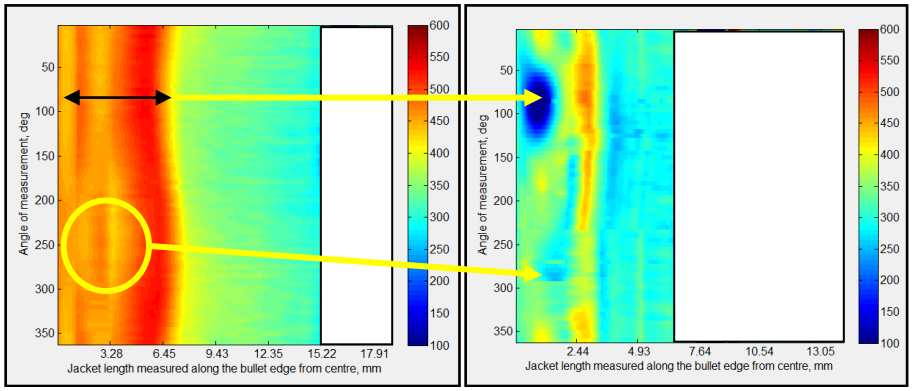

Figure 13. Bullet 16 Cartesian Plots (undeformed & deformed)

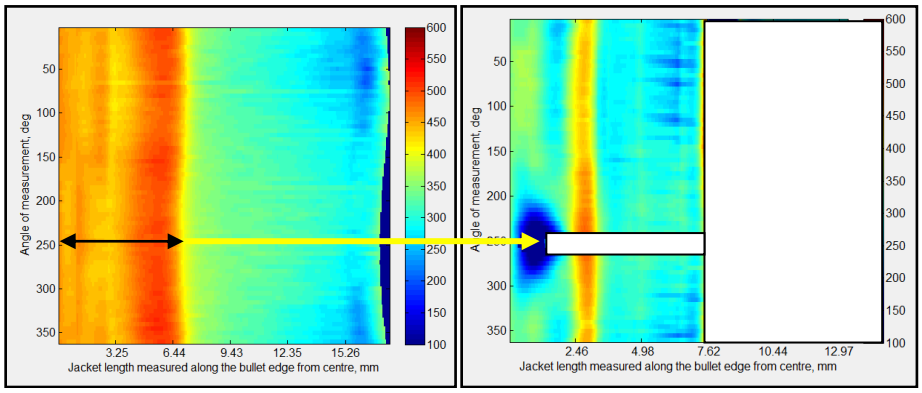

Figure 14. Bullet 17 Cartesian and Polar Cartesian Plots (undeformed & deformed)

The RWS bullet heads did not show the distinct 'ring' seen in the GM bullet heads. But the deformed plots again show distinct areas of thinning. There is a correlation between the angular position of the thinning in the deformed bullets and the shortest length of the area of increased jacket thickness in the un-deformed bullets.

6. CONCLUSIONS

This study applies the non-destructive X-ray Computed Tomography (CT) method developed by Kumar et al. to bullets that have been impact tested. A set of 20 bullets (9mm DM11) were tested and thickness variations of the order of 200µm along the length were found commonly across all of the bullets and angular variations of up to 50µm were found in a several.

The study highlights the difficulty in achieving consistent bullet velocities. Trends have been identified, but for a more detailed and conclusive analysis more tests will be required. Of the two different DM11 bullet specifications tested, the GM bullet heads provided the most consistent bullet velocities. This is most likely because of a better compatibility with the casings used in this test series.

A measure of the bullet mechanical compliance is the movement of the bullet calculated COG on impact. The study of the small batch of valid (i.e. similar velocities) results suggests that larger bullet deformations correspond to lower minimum jacket thicknesses. Thinning that can lead to rupture has been shown to be influenced by jacket thickness variations and the most likely area for rupture of the jacket is affected by the radial forces transferred between the bullet tip and target. This suggests that manufacturing tolerances and inter-manufacturer variability are significant contributing factors to a bullet's threat level, and that jacket thickness is, perhaps, as important as bullet velocity as a performance indicator.

This method of analysis can be used to support the development of standards related to bullet characterisation in the personal protection industry. Going forward, the authors aim to use the results of this study to motivate and validate finite element modelling of ballistic impacts to feed into simulations of events such as those covered by the V50 soft armour test. If inter-manufacturer variability is found to be as significant as is believed, then it could serve to call for more stringent quality control in the ammunition used for such tests in the future.

Acknowledgements

The authors would like to thank Jagadeesha Kumar, Daniel Norman, Karol Tomczyk and Ian McDonnell for their contributions to the CT image processing and analysis framework, and to Peter Hall at Hallrite Precision Engineering for his assistance with ballistic tests. This work is carried out as part of the PVCIT Centre of Excellence Research Centre, part funded by Advantage West Midlands and the European Regional Development Fund.

References

[1] Kumar J. et al, Inconsistency in 9mm bullets measured with non-destructive X-ray computer tomography, *Forensic Sci. Int.*, 214 (2011), 48-58.
[2] Knudsen P. and Theilade P., Terminal ballistics of the 7.62 mm NATO bullet autopsy findings, *International Journal of Legal Medicine*, 106 (2) (1993), 61-67
[3] Gotts P. et al, Variations in ammunition used for testing personal armour, Personal Armour Systems Symposium (PASS 2010), Quebec, Canada, Sep 13-17, 2010.
[4] Bixter R.P. et al, Bullet identification with radiography, *Radiology*, 178 (1991), 563-567.
[5] Dodd III G.D. and Budzik Jr R.F., Identification of retained firearm projectiles on plain radiographs, *AJR*, 154 (1990), 471-475.
[6] Mary-Jacque M. et al, Firearms examinations by scanning electron microscopy: observations and an update on current and future approaches, *AFTE Journal*, 24 (3) (1992), 294-303.
[7] Brandone A. and Piancone G.F., Characterisation of firearms and bullets by instrumental neutron activation analysis, *The International Journal of Applied Radiation and Isotopes*, 35 (5) (1984), 359-364.
[8] Kak A.C. and Slanley M., *Principles of computed tomography imaging*, (IEEE Publishing, New York, 1999)
[9] Kumar J. et al, Analysis of the effect of cone-beam geometry and test object configuration on the measurement accuracy of a computed tomography scanner used for dimensional measurement, *Measurement Science and Technology*, 22 (3) (2011), 035105